



## Studies on the Removal of Basic Fuchsin Dye from Aqueous Solution by HCl Treated Malted Sorghum Mash

E.O. Oyelude\*, F. Frimpong, D. Dawson

Department of Applied Chemistry and Biochemistry, University for Development Studies  
P.O. Box 24, Navrongo, Upper East Region, Ghana

Received 02 Oct 2014, Revised 1 Dec 2014, Accepted 1 Dec 2014

\*Corresponding Author: E-mail: [emmanola@gmail.com](mailto:emmanola@gmail.com) ; Tel: +233 24668 1133

### Abstract

The efficacy of using HCl-modified malted sorghum mash to remove basic fuchsin dye from aqueous solution was investigated through batch adsorption studies. The quantity of dye removed by the adsorbent increased with increase in contact time and optimum adsorption was achieved in 30 min. The adsorption process was dependent on pH of aqueous solution with optimum removal of dye occurring between pH = 4 and pH = 9. The adsorption of dye by the adsorbent increased with increase in initial dye concentration but decreased with an increase in adsorbent dose. Adsorption equilibrium data were fitted with Langmuir, Freundlich, Dubinin-Radushkevich and Temkin equations to describe the isotherms. The Langmuir and Temkin models described the experimental data better than the Dubinin-Radushkevich and Freundlich models. The maximum adsorption capacity of HCl-modified malted sorghum mash was  $58.48 \text{ mg.g}^{-1}$  at 304 K. The kinetic data were fitted with the pseudo-first order, pseudo-second order, intraparticle diffusion and Elovich models. The pseudo-second order model yielded a much better fit than the other kinetic models. The free energy of adsorption ( $\Delta G^\circ$ ) was evaluated as  $-22.54 \text{ kJ.mol}^{-1}$ . The negative value of  $\Delta G^\circ$  confirmed the feasibility of the process and the spontaneous nature of adsorption.

**Keywords:** Adsorption, Malted sorghum mash, Basic fuchsin, Isotherms, Kinetics, Thermodynamics

### 1. Introduction

The processes available for treating colored wastewater include: cation exchange membranes, photocatalytic degradation, sonochemical degradation, electrochemical degradation, micellar enhanced ultra-filtration, solar photo-Fenton and biological processes, Fenton-biological treatment scheme, adsorption/precipitation processes and adsorption on activated carbon, among others [1]. Adsorption process using activated carbon is a popular process. However, commercial activated carbon is very expensive and the need to regenerate it after use further adds to the cost of treatment. These challenges have encouraged research into low-costs for treating water and wastewater. Researchers have shown that plant-based adsorbents which are cheap, renewable and biodegradable may be promising alternatives to commercial activated carbon. Some of the plant-based adsorbents that have been studied for removal of dyes from aqueous solution include: pineapple stem [1], neem leaf powder [2], *Calotropis procera* leaf powder [3], palm kernel fibre [4], waste tea [5], coniferous pinus bark powder [6], and jack fruit peel [7].

Malted sorghum mash is a by-product of local fermented sorghum beverage, called *pito*, produced in northern Ghana. *Pito* is similar to traditional *burukutu* brewed in northern Nigeria and *dolo* brewed in Burkina Faso [8 and 9]. The mash is often fed to livestock or disposed as waste after *pito* production. The aim of this research was to investigate the potential of using hydrochloric acid modified malted sorghum mash as an adsorbent for removing basic fuchsin dye from aqueous solution.

### 2. Materials and Methods

#### 2.1 Materials

Malted sorghum mash was obtained from a local sorghum beer brewery at Navrongo, Upper East Region, Ghana. The mash was washed thoroughly with tap water until the wash water was colorless; and later rinsed thrice with

large volume of distilled water. The mash was dried to constant weight in an oven at a temperature of 333 K. The adsorbent was modified by the method of Oyelude and Owusu [3] to produce HCl-modified mash (HMM). The HMM was washed with distilled water to neutral pH and dried to constant weight at 333 K [10]. It was then ground to pass through a 2 mm sieve and stored in an air-tight bottle.

Basic fuchsin (BF) dye used was produced by Sigma-Aldrich. Its molecular formula, molecular weight, color index (CI) and maximum wavelength ( $\lambda_{\max}$ ) are:  $C_{20}H_{20}ClN_3$ , 337.5 g.mol<sup>-1</sup>, 42510 and 550 nm; respectively. The dye was used as supplied without any purification. The stock solution of BF (1000 mg.L<sup>-1</sup>) was prepared and the dye solution used for the experiments was prepared by diluting the stock solution as needed.

## 2.2 Adsorption Studies

Batch adsorption experiments were performed at average room temperature of 304±1 K to study the effect of contact time, pH of BF solution, HMM dose, temperature, and initial concentration of dye, on adsorption. 0.50 g of HMM was put in a set of 250 ml conical flasks each containing 25 ml of dye solution. The flasks were placed on a mechanical shaker and agitated at 120 rpm until equilibrium was attained. The effect of pH was studied by varying pH of BF solution from 2 to 12. The pH of the solution was adjusted using either 0.10 M HCl or 0.10 M NaOH. The effect of dosage was studied by varying the mass of HMM from 0.05 g to 0.40 g. The effect of temperature on adsorption was carried out using an isothermal water bath set at 298 K, 304 K and 313 K. The effect of dye concentration on adsorption was studied by varying dye concentration from 50 to 400 mg.L<sup>-1</sup>. Every adsorption experiment was carried out at least thrice, and blank experiments were carried out without HMM to account for dye that might stick to the flask.

At the end of each adsorption experiment, the mixture of HMM and BF was centrifuged at 4000 rpm for 5 min. The absorbance of residual dye was measured at 550 nm using UV-visible spectrophotometer (SMPC 22) and its concentration calculated as appropriate. The quantity of dye adsorbed at equilibrium,  $Q_e$  (mg.g<sup>-1</sup>), was calculated using the following relationship:

$$Q_e = \frac{(C_o - C_e)V}{w} \quad (1)$$

Where  $C_o$  and  $C_e$  (mg.L<sup>-1</sup>) are the initial and equilibrium concentration of dye, respectively;  $V$  (L) is the volume of dye solution and  $w$  (g) is the mass of HMM. The amount of dye removed (%) was calculated as follows:

$$\text{Dye removed (\%)} = \frac{(C_o - C_t)100}{w} \quad (2)$$

where  $C_t$  (mg.L<sup>-1</sup>) is the residual dye at time  $t$  (min).

The kinetic of adsorption was studied using BF of initial concentration of 50, 100, 200, 300 and 400 mg.L<sup>-1</sup>. A typical experiment was conducted by weighing 0.50 g of HMM into eight conical flasks each containing 25 mL of BF solution. The flasks were agitated as described earlier and the residual dye concentration in the flasks was determined at 5 min intervals to deduce the amount of BF adsorbed by HMM.

## 3. Results and Discussion

### 3.1 Equilibrium Adsorption

The result of the effect of contact time on the adsorption of BF is shown in Fig. 1. For a given initial concentration of BF, the quantity of BF adsorbed increased with time until the equilibrium time of 30 min was attained. Further agitation beyond this time did not lead to any increase in the adsorption of the dye. On the basis of this result, the rest of the adsorption experiments were conducted by shaking the BF-HMM system at 120 rpm for 60 min. There seemed to be high affinity for BF by HMM because of the short time for the process to attain equilibrium [3].

The effect of pH on the adsorption of BF is presented in Fig. 2. Optimum dye adsorption occurred from pH = 4 to pH = 9, and the quantity of BF adsorbed by HMM decreased sharply below pH = 4 and beyond pH = 9. The pH of an adsorbate solution has an impact on the charge properties of the adsorbent [11]. The low adsorption of BF by HMM at pH below 4 might be as a result of repulsion between the net positive surface charge of the HMM and the cationic BF. This is equally true at pH higher than 9 when the net charge on the surface of the adsorbent tends to be positive leading to reduction in the quantity of dye adsorbed [6]. Hameed [7] who studied the effect of pH on the adsorption of methylene blue by jackfruit peel obtained similar result.

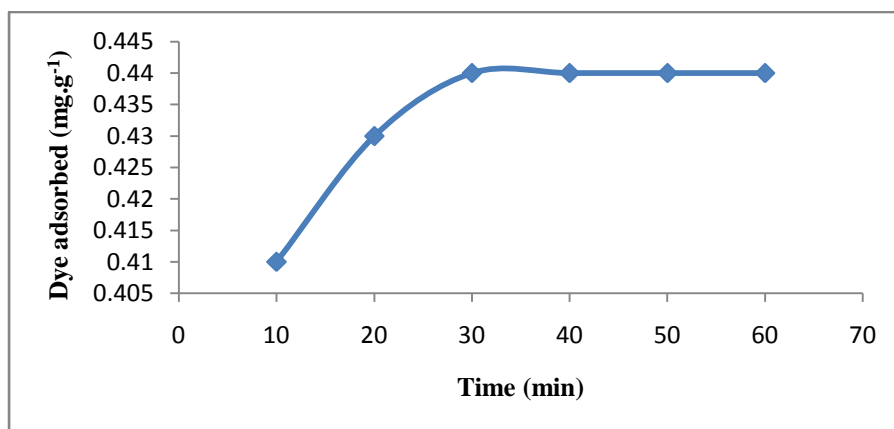


**Figure 1:** Effect of contact time on adsorption of BF by HMM (C<sub>0</sub> = 10 mg.L<sup>-1</sup>).

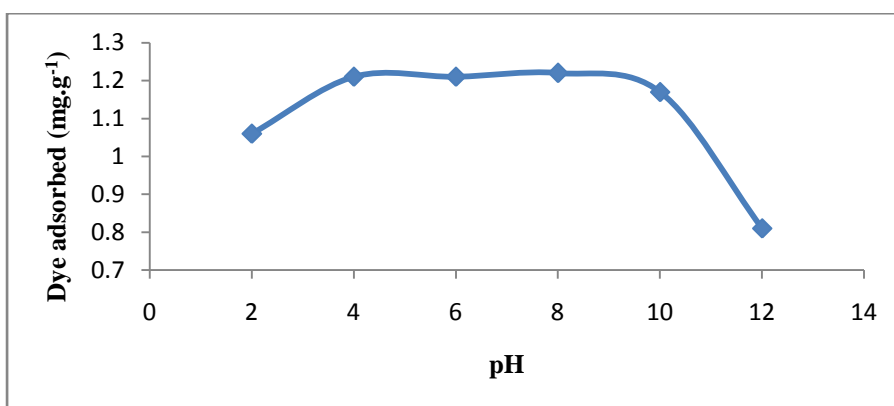


**Figure 2:** Effect of pH on adsorption of BF by HMM (C<sub>0</sub> = 25 mg.L<sup>-1</sup>).

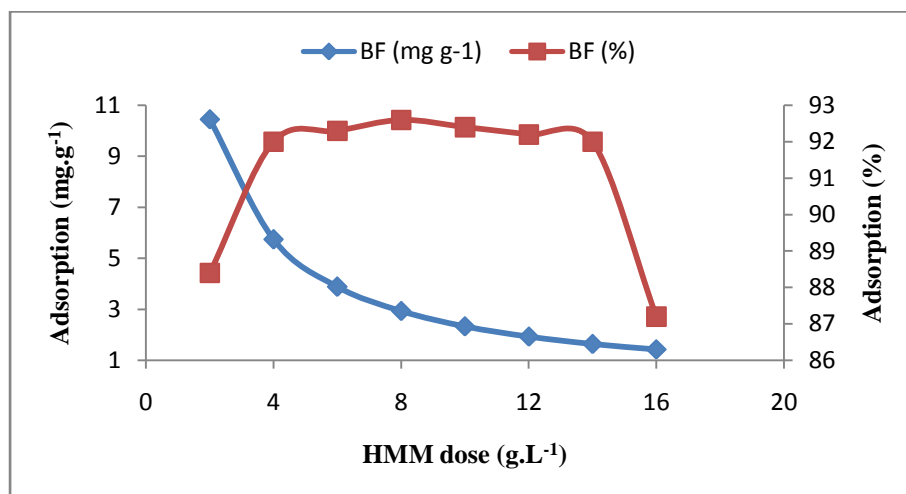


**Figure 3:** Effect of HMM dosage on adsorption of BF (C<sub>0</sub> = 25 mg.L<sup>-1</sup>).

The result of the effect of adsorbent dose on adsorption is shown in Fig. 3. The quantity of dye (on percentage basis) removed from aqueous solution increased with increase in adsorbent dosage reaching optimum level at 8 g.L<sup>-1</sup>. The uptake of dye in aqueous solution decreased when the adsorbent dosage was greater than 8 g.L<sup>-1</sup>.

However, the quantity of dye adsorbed at equilibrium for the removal of BF from aqueous solution decreased from 10.45 mg.g<sup>-1</sup> to 1.43 mg.g<sup>-1</sup> when adsorbent dosage was increased from 2 g.L<sup>-1</sup> to 16 g.L<sup>-1</sup>. At higher adsorbent to solute concentration ratios, there was a very fast superficial adsorption onto the adsorbent surface that produced a lower solute concentration in the solution than when the biomass to solute concentration ratio was lower. Thus, with increasing mass of adsorbent, the amount of dye adsorbed onto unit weight of adsorbent reduced causing a decrease in equilibrium adsorption density. HMM dosage should be 3 g.L<sup>-1</sup> or lesser to avoid wastage of adsorbent. This information is important to design economical and large scale adsorption devices [12]. The effect of initial BF concentration on the removal of the dye from aqueous solution by HMM is presented in Fig. 4. The amount of dye adsorbed increased with increased dye concentration.

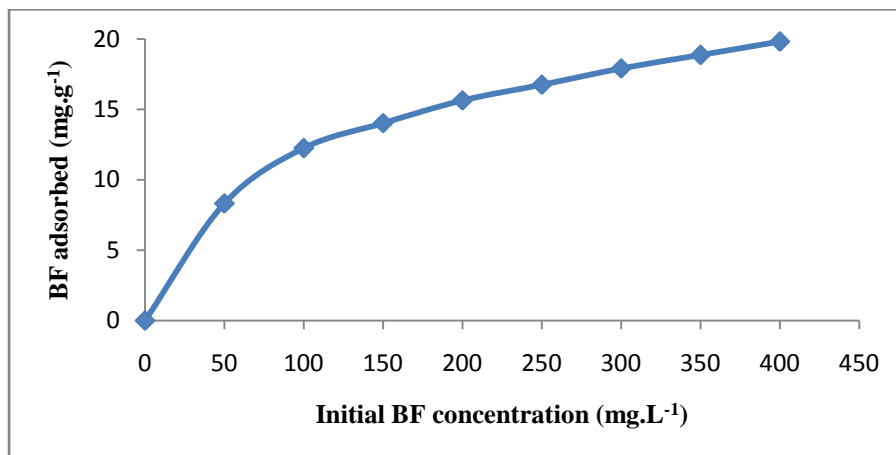


**Figure 4:** Effect of initial BF concentration on adsorption of BF.

The equilibrium adsorption capacity of BF by HMM increased from 8.33 mg.g<sup>-1</sup> to 19.80 mg.g<sup>-1</sup> when the initial concentration of BF was increased from 50 mg.L<sup>-1</sup> to 400 mg.L<sup>-1</sup>. The increase in adsorption of BF is due to the availability of more dye molecules for the limited binding sites on the adsorbent surface [5].

The effect of temperature on the uptake of BF by HMM was studied from 298 K to 313 K (figure not shown). The effect of temperature on adsorption was not obvious at initial dye concentrations below 350 mg.L<sup>-1</sup>. However, at higher dye concentrations, the equilibrium adsorption capacity of dye increased as temperature was raised from 298 K to 313 K. This implies that the removal of BF molecules from aqueous solution by HMM was endothermic in nature.

### 3.2 Adsorption Isotherm

Adsorption isotherm indicates how adsorbate molecules distribute between the liquid phase and solid phase at equilibrium. It is very important in describing the adsorption process, and for designing adsorption system [6]. Langmuir, Freundlich, Temkin and Dubinin-Radushkevich adsorption isotherm models were employed to establish the most appropriate correlations for the equilibrium data.

The Langmuir model [13] assumes monolayer adsorption onto an adsorbent surface containing a finite number of adsorption sites. The linear form of the Langmuir equation is

$$\frac{C_e}{Q_e} = \left(\frac{1}{bQ_m}\right) + \left(\frac{1}{Q_m}\right)C_e \quad (3)$$

where  $C_e$  (mg.L<sup>-1</sup>) is the equilibrium concentration of the dye,  $Q_e$  (mg.g<sup>-1</sup>) is the dye adsorbed per unit mass of HMM,  $b$  (L.mg<sup>-1</sup>) is the Langmuir adsorption constant and  $Q_m$  (mg.g<sup>-1</sup>) is the theoretical maximum adsorption capacity. The plot of specific adsorption ( $C_e/Q_e$ ) against the equilibrium concentration ( $C_e$ ) is presented in Fig. 5.

The Langmuir constants  $b$  and  $Q_m$  were determined from the slope and intercept of the plot and are presented in Table 1. The essential characteristics of the Langmuir isotherm can be expressed in terms of a dimensionless constant separation factor  $R_L$  [14] given by:

$$R_L = \frac{1}{1 + bC_0} \quad (4)$$

where  $C_0$  ( $\text{mg L}^{-1}$ ) is the highest initial concentration of BF and  $b$  ( $\text{L.mg}^{-1}$ ) is the Langmuir adsorption constant. The range of  $R_L$  value can be used to classify adsorption as follows: irreversible adsorption ( $R_L = 0$ ), favorable adsorption ( $0 < R_L < 1$ ), linear adsorption ( $R_L = 1$ ), and unfavorable adsorption ( $R_L > 1$ ). The  $R_L$  values for the removal of BF by HMM were in the range of  $0 < R_L < 1$  implying favourable adsorption process.

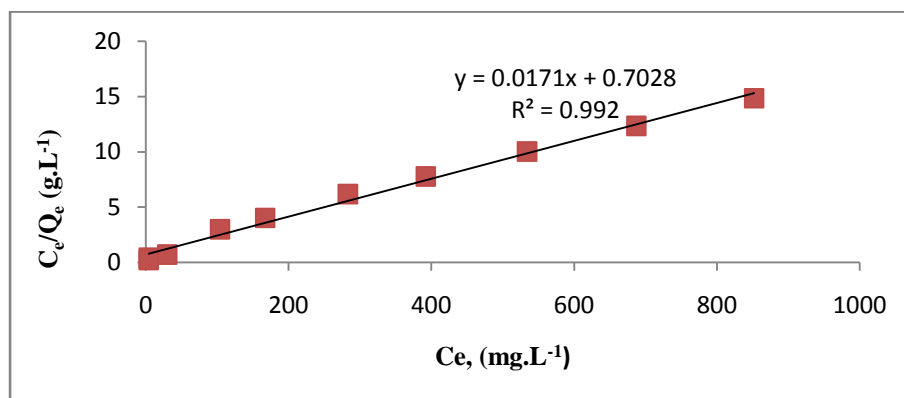


**Figure 5:** Langmuir isotherm for adsorption of BF onto HMM ( $T = 304$  K).

The Freundlich isotherm assumes multilayer adsorption on heterogeneous surface [15]. The amount of dye adsorbed increases indefinitely with an increase in concentration. The linearized Freundlich equation can be written as:

$$\log Q_e = \log K_F + \left(\frac{1}{n}\right) \log C_e \quad (5)$$

where  $Q_e$  ( $\text{mg.g}^{-1}$ ) is the dye adsorbed at equilibrium,  $C_e$  ( $\text{mg.L}^{-1}$ ) is the equilibrium concentration of BF,  $K_F$  ( $\text{mg.g}^{-1} (\text{L.mg}^{-1})^{1/n}$ ) and  $1/n$  are constants of adsorption capacity and adsorption intensity, respectively [1]. The values of  $K_F$  and  $n$  are calculated from the intercept and slope of the plot (Fig. 6) and are listed in Table 1.

Temkin isotherm assumes that the heat of adsorption of all the molecules in the layer decreases linearly with coverage due to adsorbate species. Adsorbent interactions and adsorption is characterized by a uniform distribution of binding energies, up to some maximum binding energy.

$$Q_e = \beta \ln K_T + \beta \ln C_e \quad (6)$$

where,  $\beta = RT/b$  is the constant representing the heat of adsorption and  $K_T$  ( $\text{L.mg}^{-1}$ ) is the equilibrium binding constant or maximum binding energy,  $T$  (K) is the absolute temperature,  $R$  ( $8.314 \text{ J.mol}^{-1} \text{ K}^{-1}$ ) is the universal gas constant [12]. Temkin constants are obtained from the plot of  $Q_e$  against  $\ln C_e$  (Fig. 7) and are listed in Table 1.

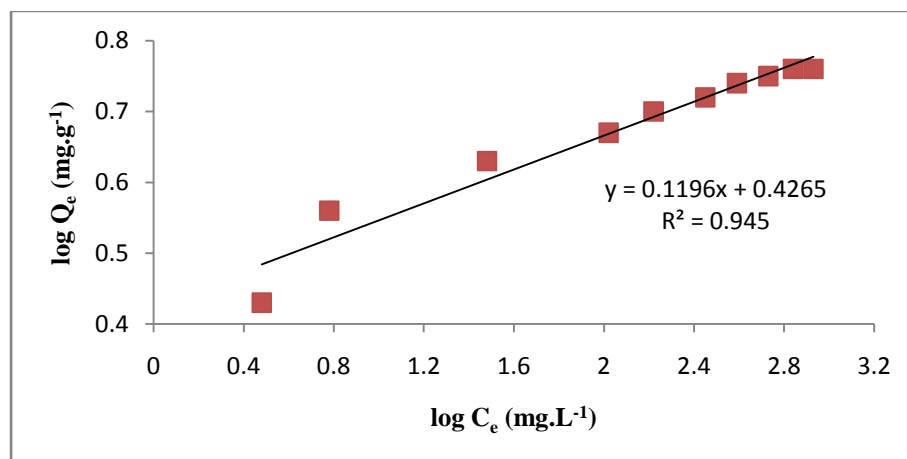


**Figure 6:** Freundlich isotherm for adsorption of BF onto HMM ( $T = 304$  K).

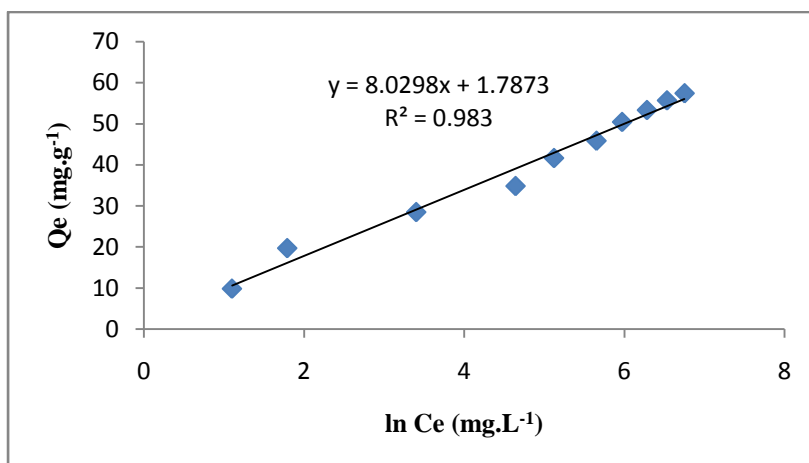


**Figure 7:** Temkin isotherm for adsorption of BF onto HMM (T = 304 K).

The Dubinin-Radushkevich isotherm model [16] finds application in the determination of whether an adsorption process is physical or chemical in nature. The model is employed to estimate the porosity and the apparent free energy of adsorption. The Dubinin-Radushkevich equation [5] is given by:

$$Q_e = Q_m \exp(-\beta \epsilon^2) \quad (7)$$

where  $Q_e$  (mg.g<sup>-1</sup>) is the dye adsorbed at equilibrium,  $Q_m$  (mg.g<sup>-1</sup>) is the maximum adsorption capacity,  $\beta$  (mol<sup>2</sup>.J<sup>-2</sup>) is the activity coefficient related to adsorption mean free energy and  $\epsilon$  (J.mol<sup>-1</sup>) is the Polanyi potential written as:

$$\epsilon = RT \ln \left( 1 + \frac{1}{C_e} \right) \quad (8)$$

The linear expression of the Dubinin-Radushkevich equation [17, 18] is:

$$\ln Q_e = \ln Q_m - 2\beta \epsilon^2 \quad (9)$$

The values of  $Q_m$  and  $\beta$  (Table 1) are determined from the plot of dye adsorbed at equilibrium ( $Q_e$ ) against  $\epsilon$  (Fig. 8). The mean free energy (J.mol<sup>-1</sup>) of adsorption is calculated from the relationship:

$$E = \frac{1}{(2\beta)^{0.5}} \quad (10)$$

The mean adsorption free energy for physical and chemical mechanisms are given by  $0 < E < 8000$  J.mol<sup>-1</sup> and  $8000 < E < 16000$  J.mol<sup>-1</sup>, respectively [5]. The calculated mean free energy of adsorption was 22.36 J.mol<sup>-1</sup>. Therefore, the adsorption mechanism is physical in nature.

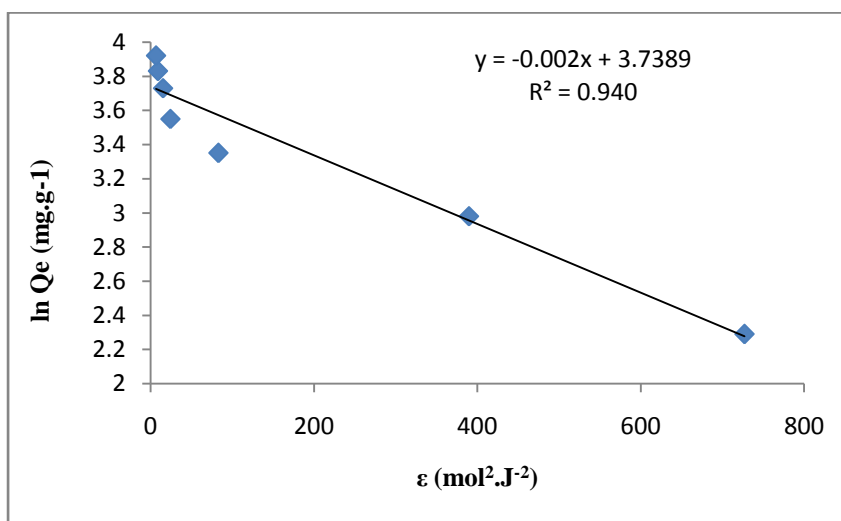


**Figure 8:** Dubinin-Radushkevich isotherm for adsorption of BF onto HMM (T = 304 K).

**Table 1:** Isotherm parameters for adsorption of BF onto HMM at 304 K

Isotherm	Parameter	Value
Langmuir	$Q_m$ (mg.g <sup>-1</sup> )	58.48
	$b$ (L m.g <sup>-1</sup> )	0.024
	$R^2$	0.992
Freundlich	$K_F$	2.670
	$1/n$	0.120
	$R^2$	0.945
Temkin	$K_T$	1.249
	$\beta$	8.030
	$R^2$	0.983
Dubinin-Radushkevich	$Q_m$ (mg.g <sup>-1</sup> )	42.05
	$\beta$ (mol <sup>2</sup> .J <sup>-2</sup> )	$1.0 \times 10^{-3}$
	$E$ (J.mol <sup>-1</sup> )	22.36
	$R^2$	0.940

It is clear from the information in Table 1 that Langmuir isotherm ( $R^2 = 0.992$ ) best fit the adsorption process; followed by Temkin isotherm ( $R^2 = 0.983$ ), Freundlich isotherm ( $R^2 = 0.942$ ) and Dubinin-Radushkevich isotherm ( $R^2 = 0.940$ ) in that order.

### 3.3 Adsorption Kinetics

The kinetics of adsorption of an adsorbate by any adsorbent is required for selecting optimum operating conditions for the full-scale batch process [19]. Four models were applied to test experimental data and thus elucidate the kinetic of the adsorption process. The linearized form of the Lagergren [20] pseudo-first order equation is expressed as follows:

$$\log(Q_e - Q_t) = \log Q_e - \left(\frac{k_1}{2.303}\right)t \quad (11)$$

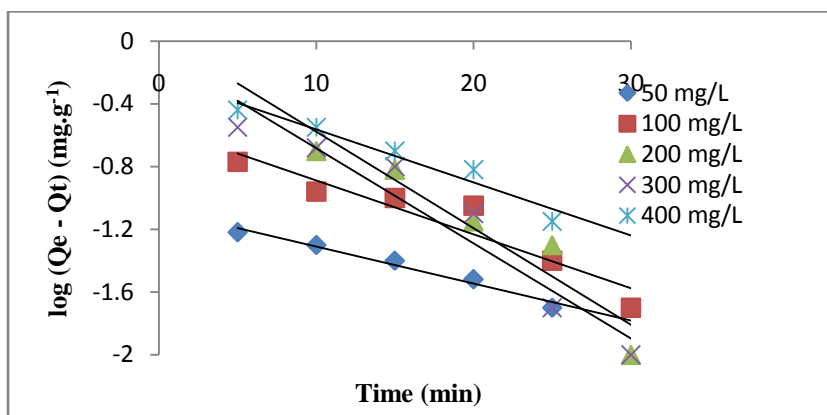


**Figure 9:** Pseudo-first order kinetics for adsorption of BF onto HMM (T = 304 K).

where  $Q_t$  (mg.g<sup>-1</sup>) is the amount of adsorbate adsorbed at any time,  $Q_e$  (mg.g<sup>-1</sup>) is the amount of adsorbate adsorbed at equilibrium,  $t$  (min) is time and  $k_1$  (L.min<sup>-1</sup>) is the rate constant. The rate constant was obtained from the plot of  $\log(Q_e - Q_t)$  against  $t$  (Fig. 9). The calculated values of  $Q_e$ ,  $k_1$  and the correlation coefficient ( $R^2$ ) are listed in Table 2.

The pseudo-second order kinetics equation is often successfully used to model the adsorption of adsorbate by adsorbent surface [21]. The pseudo-second order equation is:

$$\frac{t}{Q_t} = \frac{1}{k_2 Q_e^2} + \left(\frac{1}{Q_e}\right)t \quad (12)$$

where  $k_2$  ( $\text{g} \cdot \text{mg}^{-1} \cdot \text{min}^{-1}$ ) is the rate constant of adsorption,  $Q_e$  ( $\text{mg} \cdot \text{g}^{-1}$ ) is the amount of BF adsorbed at equilibrium and  $Q_t$  ( $\text{mg} \cdot \text{g}^{-1}$ ) is the amount of adsorbed dye at time  $t$  (min). The equilibrium constant is calculated from the plot of  $t/Q_t$  against  $t$  (Fig. 9). The generated values of  $Q_e$ ,  $k_2$  and  $R^2$  are presented in Table 2.

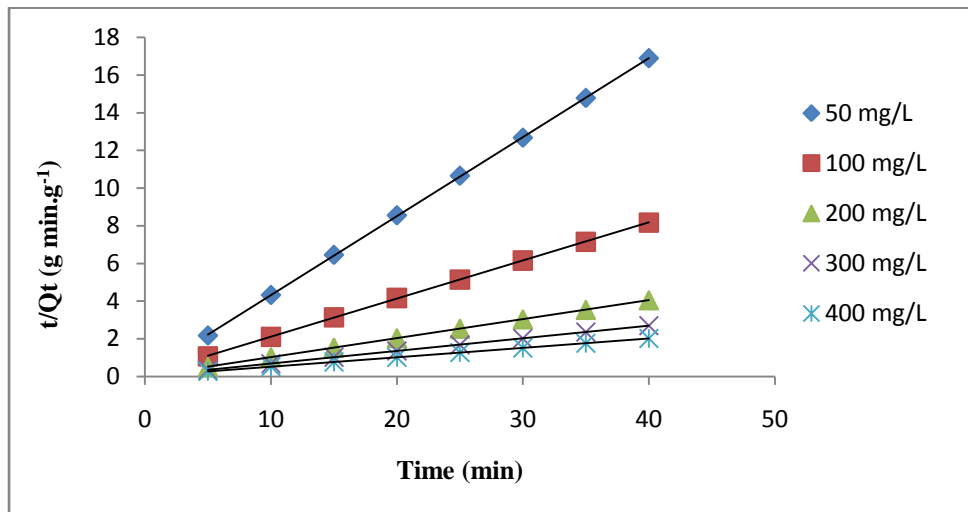


Figure 10: Pseudo-second order kinetics for adsorption of BF onto HMM (T = 304 K).

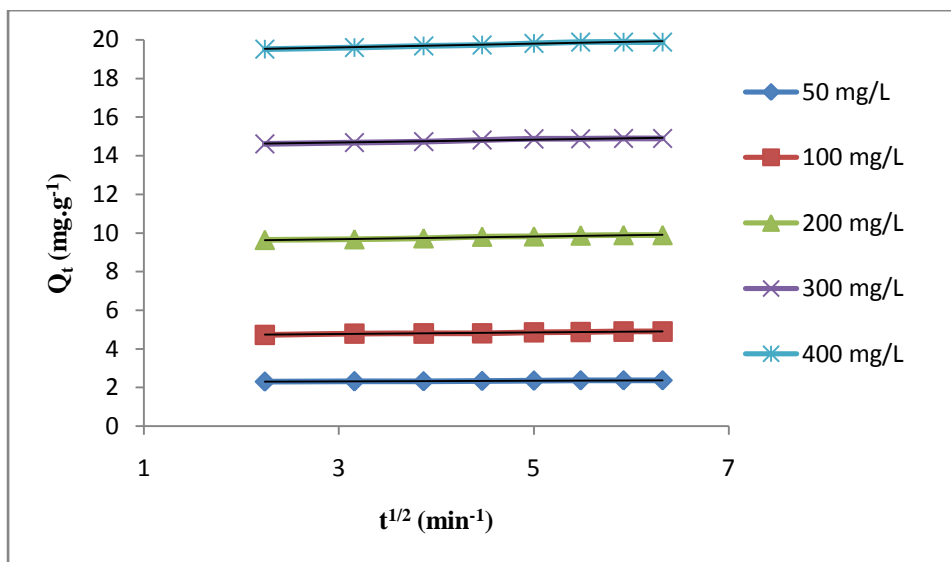


Figure 11: Intraparticle diffusion kinetics for adsorption of BF onto HMM (T = 304 K).

The intraparticle diffusion kinetic model is given by the relationship:

$$Q_t = k_i t^{1/2} + C \quad (13)$$

where  $C$  is the intercept and  $k_p$  is the intraparticle diffusion rate constant ( $\text{mg} \cdot \text{g}^{-1} \cdot \text{min}^{1/2}$ ), the values of  $k_i$  give an idea about the boundary layer thickness (Fig. 11). The intercept is directly proportional to the boundary layer effect [22]. There is only one linear portion for every studied concentration of BF which implies that intraparticle diffusion contributes significantly to the adsorption of BF by HMM. The deviation of the lines from the origin may be because of the difference in the rate of mass transfer in the initial and final stages of adsorption [23]. Furthermore, the deviation of the lines from the origin indicates that intraparticle diffusion was not the only rate-limiting step. It is likely that surface adsorption played some role in the adsorption of BF by HMM [24]. The values of  $k_i$ ,  $C$  and  $R^2$  are presented in Table 2.



Elovich model is used to describe second-order kinetic by assuming that the adsorbent surface is energetically heterogeneous [25]. Simple Elovich model is represented by the relationship:

$$Qt = \alpha + \beta \ln t \quad (14)$$

where  $\alpha$  ( $\text{mg.g}^{-1} \text{min}^{-1}$ ) is the initial adsorption rate constant and  $\beta$  ( $\text{g.mg}^{-1}$ ) is the initial desorption rate constant. A plot of  $Qt$  versus  $\ln t$  (figure not shown) gives a linear relationship if the model is applicable to the model [11]. The values of  $\alpha$ ,  $\beta$  and  $R^2$  generated are presented in Table 2.

The comparison of the four selected kinetic models showed that pseudo-second order model with the highest correlation coefficient values best describe the adsorption process. Moreover, the generated experimental values of adsorption capacity were much closer to the theoretical values [5, 26].

**Table 2:** Kinetic parameters for adsorption of BF onto HMM at 304 K

Pseudo-First Order			
$C_o$ ( $\text{mg.L}^{-1}$ )	$Q_e$ ( $\text{mg.g}^{-1}$ )	$k_1$ ( $\text{min}^{-1}$ )	$R^2$
50	11.858	0.054	0.975
100	3.5051	0.079	0.896
200	1.0914	0.142	0.906
300	1.1948	0.140	0.930
400	1.6788	0.078	0.946
Pseudo-Second Order			
$C_o$ ( $\text{mg L}^{-1}$ )	$Q_e$ ( $\text{mg.g}^{-1}$ )	$k_2$ ( $\text{mg.g}^{-1} \text{min}^{-1}$ )	$R^2$
50	2.3849	1.514	1.000
100	4.9407	0.541	0.999
200	9.9206	0.546	1.000
300	14.925	0.483	1.000
400	20.000	0.250	1.000
Intraparticle Diffusion			
$C_o$ ( $\text{mg.L}^{-1}$ )	$k_i$ ( $\text{mg.g}^{-1} \text{min}^{-1/2}$ )	$C$ ( $\text{mg.g}^{-1}$ )	$R^2$
50	0.0167	2.269	0.959
100	0.0426	4.640	0.964
200	0.0684	9.481	0.971
300	0.0754	14.451	0.948
400	0.0974	19.304	0.971
Elovich			
$C_o$ ( $\text{mg.L}^{-1}$ )	$\alpha$ ( $\text{mg.g}^{-1}$ )	$\beta$ ( $\text{mg.g}^{-1} \text{min}^{-1}$ )	$R^2$
50	44.991	0.650	0.917
100	91.721	1.679	0.937
200	187.30	2.871	0.978
300	286.85	3.073	0.961
400	383.55	3.873	0.958

### 3.4 Adsorption Thermodynamic

The free energy of adsorption ( $\Delta G^\circ$ ) can be related with the equilibrium constant  $K$  ( $\text{L.mol}^{-1}$ ) by the following equation:

$$-\Delta G^\circ = RT \ln K_L \quad (15)$$

where,  $R$  represents the gas constant ( $8.314 \text{ J.mol}^{-1} \text{K}^{-1}$ ),  $T$  is the absolute temperature (K) and  $K_L$  is the Langmuir equilibrium constant. The change in enthalpy ( $\Delta H^\circ$ ) and change in entropy ( $\Delta S^\circ$ ) is calculated using the following relationship:

$$K_L = \left(\frac{\Delta S^\circ}{R}\right) - \frac{\Delta H^\circ}{R} \left(\frac{1}{T}\right) \quad (16)$$

The plot of  $\ln K_L$  against  $1/T$  at three different temperatures is presented in Fig. 12. The values of  $\Delta S^\circ$  and  $\Delta H^\circ$  are calculated from the slope and intercept on the  $\ln K_L$  axis. The values of  $\Delta G^\circ$ ,  $\Delta H^\circ$  and  $\Delta S^\circ$  are presented in Table 3. The calculated values of the thermodynamic parameters are low, which may imply that the adsorption process was spontaneous and physical in nature [25]. The negative values of  $\Delta G^\circ$  confirmed the spontaneous nature of adsorption and the feasibility of the process [27]. The heat of adsorption ( $6.65 \text{ kJ}\cdot\text{mol}^{-1}$ ) which is lesser than  $20 \text{ kJ}\cdot\text{mol}^{-1}$  confirmed that process is physical in nature [28]. The positive value of  $\Delta H^\circ$  indicates that the removal of BF from aqueous solution by HMM was an endothermic process. Chowdhury and his co-workers [29] attributed the positive value of  $\Delta S^\circ$  to imply the affinity of HMM for BF and increased randomness at the adsorbent-solution interface during adsorption.

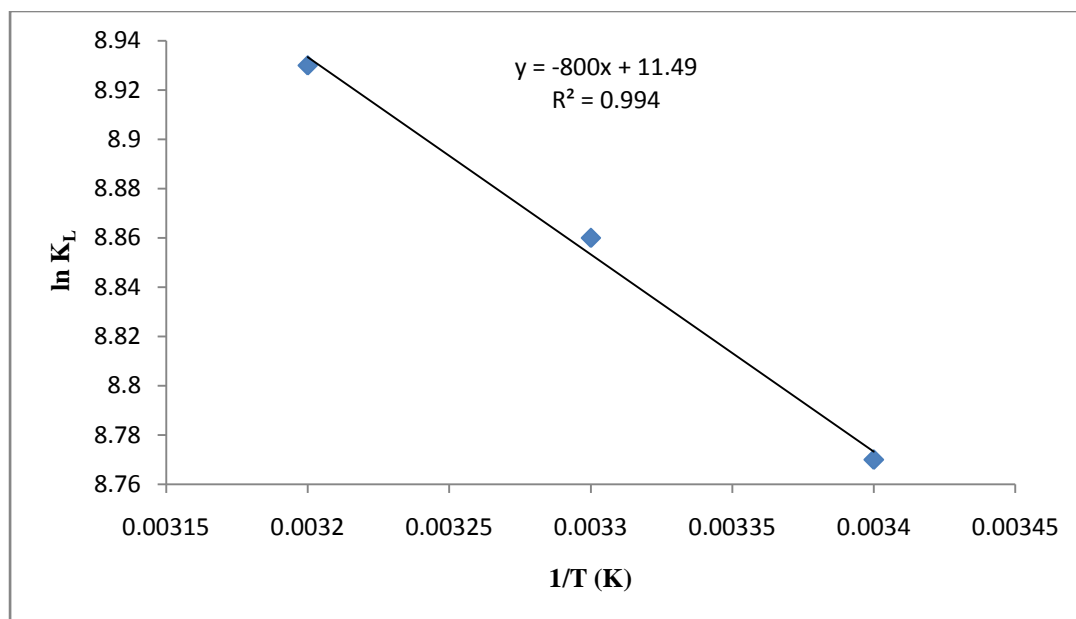


**Figure 12:** Plot of  $\ln K_L$  versus  $1/T$  for adsorption of BF onto HMM ( $T = 298, 304$  and  $313 \text{ K}$ )

**Table 3:** Thermodynamic parameters for the adsorption of BF onto HMM

T (K)	$\Delta G$ ( $\text{kJ mol}^{-1}$ )	$\Delta H$ ( $\text{kJ mol}^{-1}$ )	$\Delta S$ ( $\text{J mol}^{-1} \text{ K}^{-1}$ )
298	-21.73		
304	-22.40	6.65	95.55
313	-23.24		

## Conclusion

Batch adsorption experiments were carried out to determine the feasibility of using pulverised malted sorghum mash to remove basic fuchsin dye from aqueous solution. The adsorption process is influenced by contact time, solution pH, temperature, adsorbent dosage and concentration of the dye. The adsorption of basic fuchsin by the adsorbent was fast attaining equilibrium in just after 30 min. Optimum removal of the dye from aqueous solution occurred from pH = 4 to pH = 9 and adsorbent dosage from 2 to  $4 \text{ g}\cdot\text{L}^{-1}$ .

The adsorption isotherm for the process was best described with the Langmuir model. The calculated maximum adsorption capacity was  $58.48 \text{ mg g}^{-1}$ . The equilibrium kinetics data were best fitted with the pseudo-second order model. Intraparticle diffusion contributed significantly to the adsorption process but it is not the only rate-limiting step. The adsorption process was favorable, endothermic and physical in nature. The present study shows that malted sorghum mash may be useful as a low-cost, biodegradable, and renewable adsorbent.

## References

1. Hameed B.H., Krishni R.R., Sata S.A., *J. Hazard. Mater.*, 162 (2009) 305.
2. Bhattacharyya K.G., Sarma A., *Dyes & Pigments*, 65 (2005) 51.
3. Oyelude E.O., Owusu U.R., *J. Appl. Sci. Environ. Sanitation*, 6 (4) (2011) 477.
4. Ofomaja A.E., Ho Y.S., *Dyes & Pigments*, 74 (2007) 60.
5. Auta M., Hameed B.H., *Che. Eng. J.*, 171 (2011) 502.
6. Ahmad R., *J. Hazard. Mater.*, 171 (2009) 767.
7. Hameed B.H., *J. Hazard. Mater.*, 162 (2009) 344.
8. Sawadogo-Lingani H., Lei V., Diawara B., Nielsen D.S., Møller P.L., Traore A.S., Jakobsen M., *J. Appl. Microbiol.*, 103 (2007) 765.
9. Glover R.L.K., Sawadogo-Lingani H., Diawara B., Jespersen L., Jakobsen M., *J. Appl. Biosci.*, 22 (2009) 1312.
10. Siew T.O., Pei-Sin K., Chnoong-Kheng L., *Amer. J. Appl. Sci.*, 7 (4) (2010) 447.
11. Huang L., Kong J., Wang W., Zhang C., Niu S., Gao B., *Desalination*, 286 (2012) 268.
12. Ehrampoush M.H., Ghanizadeh G., Ghaneian M.T., *Iranian J. Environ Health Sci. & Eng.*, 8 (2) (2011) 101.
13. Langmuir I., *J. Amer. Chem. Soc.*, 40 (1918) 1361.
14. Gupta V.K., Mittal A., Gajbe V., *J. Colloid Interface Sci.*, 284 (2005) 89.
15. Hameed B.H., Din A.T.M., Ahmad A.L., *J. Hazard. Mater.*, 141 (3) (2007) 819.
16. Dubinin M.M., Radushkevich L.V., *Proc. Aca. Sci., U.S.S.R.; Phy. Chem. Section*, 55 (1947) 331.
17. Igwe J.C., Abia A.A., *Ecl. Quim.*, 32 (1) (2007) 33.
18. Ainane T., Abourriche A., Kabbaj M., Elkouali M., Bennamara A., Charrouf M., Talbi M., *J. Mater. Environ. Sci.*, 5 (4) (2014) 975.
19. Santhi T., Manonmani S., Smitha T., *J. Hazard. Mater.*, 179 (1-3) (2010) 178.
20. Lagergren S., *Kungliga Svenska Vetenskapsakademiens Handlingar*, 24 (4) (1898) 1.
21. Ghanizadeh G., Asgari G., *Reaction Kinetics, Mechanisms and Catalysis*, 102 (1) (2011) 127.
22. Bulut Y., Aydin H., *Desalination*, 194 (1-3) (2006) 259.
23. Mane V.S., Babu P.V.V., *Desalination*, 273 (2-3) (2011) 321.
24. Patil S., Deshmukh V., Renukdas S., Patel N., *Intl J. Environ Sci.*, 1 (6) (2011) 1116.
25. Silva J.P., Sousa S., Rodrigues J., Antunes H., Porter J.J., Gonçalves I., Ferreira-Dias, S., *Separation and Purification Tech.*, 40 (3) (2004) 309.
26. Fat'hi M.R., Asfaram A., Hadipour A., Roosta M., *J. Environ. Health Sci. & Eng.*, 12 (62) (2014) 1.
27. Oladoja N.A., Aboluwoye C.O., Oladimeji Y.B., *Turkish J. Eng. & Environ. Sci.*, 32 (2008) 303.
28. Naiya T.K., Bhattacharya A.K., Das, S.K., *Environ. Progress & Sustainable Energy*, 28 (4) (2009) 535.
29. Chowdhury S., Mishra R., Saha P., Kushwaha P., *Desalination*, 265 (1-3) (2011) 159.

(2015) ; <http://www.jmaterenvirosci.com>